AIP Journal of Applied Physics

Temperature dependence of full set tensor properties of KTiOPO4 single crystal measured from one sample

Yang Zhang, Liguo Tang, Nianjing Ji, Gang Liu, Jiyang Wang, Huaidong Jiang, and Wenwu Cao

Citation: Journal of Applied Physics **119**, 124104 (2016); doi: 10.1063/1.4944603
View online: http://dx.doi.org/10.1063/1.4944603
View Table of Contents: http://scitation.aip.org/content/aip/journal/jap/119/12?ver=pdfcov
Published by the AIP Publishing

JOURNAL OF APPLIED PHYSICS **119**, 124104 (2016)

Temperature dependence of full set tensor properties of $KTiOPO_4$ single crystal measured from one sample

HPSTAR 2016-184

Yang Zhang,[1,2] Liguo Tang,[2,3] Nianjing Ji,[1] Gang Liu,[4] Jiyang Wang,[1] Huaidong Jiang,[1,a)] and Wenwu Cao[2,a)]

[1]*State Key Laboratory of Crystal Materials, Shandong University, Jinan 250100, China*
[2]*Department of Mathematics and Materials Research Institute, The Pennsylvania State University, University Park, Pennsylvania 16802, USA*
[3]*Department of Applied Ocean Physics and Engineering, Xiamen University, Xiamen 361005, China*
[4]*Center for High Pressure Science and Technology Advanced Research, Shanghai 201203, China*

(Received 6 August 2015; accepted 8 March 2016; published online 23 March 2016)

The temperature dependence of the complete set of elastic, dielectric, and piezoelectric constants of $KTiOPO_4$ single crystal has been measured from 20 °C to 150 °C. All 17 independent constants for the *mm2* symmetry piezoelectric crystal were measured from one sample using extended resonance ultrasound spectroscopy (RUS), which guaranteed the self-consistency of the matrix data. The unique characteristics of the RUS method allowed the accomplishment of such a challenging task, which could not be done by any other existing methods. It was found that the elastic constants (c_{11}^E, c_{13}^E, c_{22}^E, and c_{33}^E) and piezoelectric constants (d_{15}, d_{24}, and d_{32}) strongly depend on temperature, while other constants are only weakly temperature dependent in this temperature range. These as-grown single domain data allowed us to calculate the orientation dependence of elastic, dielectric, and piezoelectric properties of $KTiOPO_4$, which are useful for finding the optimum cut for particular applications. *© 2016 AIP Publishing LLC*. [http://dx.doi.org/10.1063/1.4944603]

I. INTRODUCTION

Potassium titanyl phosphate, $KTiOPO_4$ (KTP), is one of the most widely used single crystals for laser beam control in the visible and near IR ranges,[1] especially for frequency converter in nonlinear optics. KTP is considerably superior to other well-known nonlinear optical materials for frequency doubling of continuous-wave or pulsed Nd^{3+} laser devices.[2] It possesses many outstanding properties, such as large nonlinear optical coefficients, high induced damage threshold, broad spectral bandwidth (352–4500 nm), and high chemical stability.[3,4] KTP belongs to the orthorhombic crystal class with the symmetry group *mm2*, and it has nine independent elastic constants (c_{ij}), five independent piezoelectric constants (d_{ij}), and three dielectric constants (ε_{ij}). Up to date, the temperature dependence of the complete set of elastic and piezoelectric coefficients has never been measured. It was reported that KTP has a large electromechanical coupling coefficients and its elastic constants are nearly temperature independent in the temperature range of 25–80 °C,[5] which makes it attractive for high temperature applications. Knowledge on the complete set of material property tensor is very important for in-depth theoretical analysis as well as device design using finite element simulations. Accurate elastic constants can furnish useful information about the crystal, because they are related to a variety of fundamental solid-state phenomena, such as specific heat, Debye temperature, etc.;[6] hence, it is very important to obtain the full tensor properties of KTP single crystals. The reason these tensor properties have not been measured up to date is because the task is extremely challenging. There are total 17 independent material constants to be determined. Using the IEEE impedance resonance method for such purpose needs at least 7 samples with very different geometries. Uncertainties will be introduced due to the property variation from sample to sample and the geometry dependence of properties, which makes it very difficult to achieve self-consistency of the final matrix data.

The resonant ultrasound spectroscopy (RUS) utilizes a broad resonance spectrum of coupled modes so that a lot of information can be obtained from one sample. In principle, if the mechanical quality factor Q_m is high enough,[7] it is possible to determine the full matrix constants using only one sample by solving the 3-D coupled wave equations for piezoelectric materials. Compared with the IEEE impedance resonance method of using multiple samples for such tasks, using only one sample can eliminate errors caused by sample-to-sample property variation, so that data self-consistency can be guaranteed. Tang and Cao had confirmed the validity of such data self consistency using a combination of experiments and numerical calculations.[8] Most importantly, if only one sample is needed in the extended RUS method, we could heat up this sample and obtain the temperature dependence of the RUS spectrum, which would allow us to determine the temperature dependence of the full tensor properties. This capability had already been demonstrated for measuring the temperature dependence of the full tensor properties of PZT-4 ceramics, which has 10 independent material constants.[8] It is, of course, much more challenging to get all 17 independent coefficients from one sample, which is a work to be performed here.

[a)]Authors to whom correspondence should be addressed. Electronic addresses: dzk@psu.edu and hdjiang@sdu.edu.cn

II. EXPERIMENTAL

The single crystal KTP sample used in our measurements was grown by the top seed growth method using $K_4P_2O_7$-PbO as flux. Related experimental details for the crystal growth had been reported previously.[9,10] The as grown crystal was cut into a rectangular parallelepiped along the crystallographic *x*, *y*, and *z* axes. The six faces were grinded into the final size of $5.138 \times 4.776 \times 4.606\,\text{mm}^3$. The mass of KTP sample is 0.337 g, yielding a density of $2.982\,\text{g/cm}^3$, which agrees with the previously reported value of 2.95 g/cm.[5,11] The low and high frequency capacitances from 20 °C to 150 °C were measured by an HP4294A impedance analyzer connected to a temperature chamber (Delta 9023).

There are two processes involved in the RUS method. One is the forward process, which is to use known material constants to calculate the resonance spectrum. The other is the inverse process, which is to find out the unknown material constants from the measured spectrum, which is done by incrementally adjusting the input guessing parameters and repeatedly calculating the resonance spectrum aiming to match the measured spectrum. For this reason, the parameters to be adjusted must be sensitive to the change of the spectrum. This is true for the elastic and piezoelectric constants, but not for the dielectric constants, i.e., there is little change of the spectrum when there is already a very large change of the dielectric constants. Therefore, the clamped dielectric constants ε_{11}^S, ε_{22}^S, and ε_{33}^S must be measured directly on the same sample because they cannot be measured by the RUS method due to their poor sensitivity to mechanical resonance modes.[8] The free dielectric constants ε_{11}^T, ε_{22}^T, and ε_{33}^T measured at the same time will be used later for the self-consistency check of the obtained full set data.

To reduce the difficulty of multivariable inversion problem at room temperature (T = 20 °C), the elastic stiffness constants c_{11}^E, c_{22}^E, c_{44}^E, c_{55}^E, and c_{66}^E were measured separately on the same sample using an ultrasonic pulse-echo method. A 15 MHz longitudinal wave transducer (Ultran Laboratories, Inc.) and a 5 MHz shear wave transducer (Panametrics Com.) were used in the ultrasonic pulse-echo measurements. The transducer was excited by a 200 MHz pulser/receiver (Panametrics Com.), and the echoes were received by the same transducer, and then the amplified output signals from the pulser/receiver were fed into a Tektronix 430A digital oscilloscope for measuring the time of flight between echoes. The phase velocities of the longitudinal and shear waves along the three principal axis directions could be calculated from the measured time of flight and the corresponding sample dimensions, the elastic stiffness constants c_{11}^E, c_{22}^E, c_{44}^E, c_{55}^E, and c_{66}^E were subsequently calculated from the velocities and the measured density. For example, c_{11}^E can be determined using the formula $c_{11}^E = \rho v_x^2$, where ρ is the density of the sample, and v_x is the corresponding wave velocity in the sample along the *x*-direction. For more general cases, the relationships between phase velocities and elastic constants can be found in Refs. 12 and 13.

The remaining 9 constants at room temperature can be obtained by the RUS technique. More importantly, we can use the obtained information at room temperature to identify corresponding modes in the measured resonance spectrum. These room temperature data and mode information form the basis for calculations performed at the first temperature increment ($\Delta T = 10\,°C$ in our case). In a successive manner, the temperature dependence of the full tensor properties can be derived from the same sample.

In the second stage, the resonance frequencies of the sample were measured in an air furnace (KSL 1100X) from 20 °C to 150 °C with a thermocouple placed near the sample to detect the sample temperature. The precision of the furnace temperature control is about ±0.3 °C, and the temperature step ΔT in our experiments is set to 10 °C because the temperature range is far away from the phase transition so that the temperature changes are not so drastic. A diagram of the RUS set-up is shown in Figure 1. The DRS 9000 system (Dynamic Resonance Systems, Inc.) was used to measure the resonance frequency spectrum. In the room temperature measurements, we used the transducers that came with the system, which can work from 16 kHz to 4 MHz according to the manual. We have characterized the transducers and found that their center frequency is about 30 MHz, which is far above the RUS working range. For the temperature dependence data, we made the transducers using $LiNbO_3$ single crystals. The center frequency of our transducers is about 15 MHz, which is also far above the RUS working frequency range (<2 MHz in our case). The KTP sample was mounted between the transmitting and receiving transducers, making contacts only at the opposite corners to allow free vibrations. Then, the whole assembly was placed inside the small furnace, as shown in Figure 1. The transducers were connected to the DRS 9000 system through a hole on the furnace wall using high temperature wires. We set the starting and stopping frequencies of the sweep signal to 300 kHz and 1700 kHz, respectively, and the total number of data points collected was N = 14 000, which gives a frequency resolution of 0.1 kHz. The resonance ultrasound signals were obtained by the DRS 9000 system that was controlled by a computer. A large number of vibration eigen-modes could be measured by sweeping the excitation frequencies.[14] The variational method for electroelastic vibrations was used to calculate the resonance frequencies of a rectangular parallelepiped sample.[15] Details about the RUS method and related back fitting procedure were explained in 1990 by Ohno.[16]

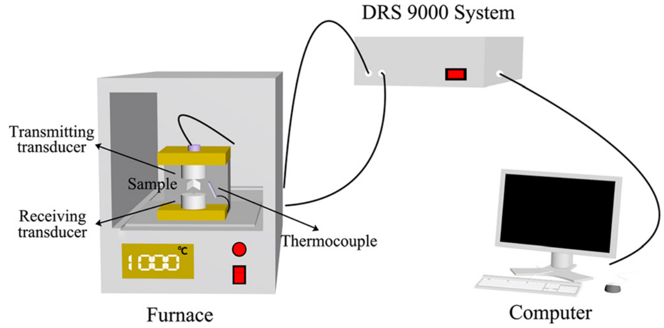

FIG. 1. The RUS experimental setup. The sample is in between the two transducers with contact at the opposite corners, and the whole assembly is inside a small furnace. The DRS 9000 is a commercial RUS system, which is controlled by a software installed in a PC.

The resonance spectra of a selected frequency range from 300 kHz to 600 kHz at 30 °C and 80 °C are shown in Figure 2. One can see that all resonance frequencies decrease with temperature for this KTP crystal.

III. RESULTS AND DISCUSSIONS

The temperature dependence of each resonance frequency, corresponding to a particular mode, was fitted to a second-degree polynomial, which can help smooth out data fluctuations. In the RUS technique, mode identification is the most difficult task when trying to extract the material constants. The final results would be wrong even if only one mode was wrongly identified. Judging by the position and interval between the resonance peaks, 109 resonant peaks from 300 kHz to 1700 kHz were identified in our case. These 109 modes were used to derive the elastic and piezoelectric constants at each temperature through the inverse calculation process.

As mentioned above, the 9 unknown elastic and piezoelectric constants at room temperature (20 °C) were first extracted using the measured resonance spectrum, then, the full tensor properties at 20 °C were used as the initial guessing parameters for the next temperature T = 30 °C. By this analogy, the inversion process was conducted every 10 °C until 150 °C. In the whole temperature range, the errors between the calculated and the measured ones for all 109 modes were below 0.35%, which gives us confidence about the obtained results.

Specifically, the inverse process is to minimize the following objective function:[17]

$$F = \sum_{i=1}^{K} w_i [f_{(cal)}^{(i)} - f_{(meas)}^{(i)}]^2, \tag{1}$$

where $f_{(cal)}^{(i)}$ and $f_{(meas)}^{(i)}$ are the computed and measured frequencies, respectively, and w_i is the weighting factor. The difference between predicted and measured frequencies can be minimized by an iterative non-linear least-squares fitting procedure, such as the Levenberg–Marquardt (LM) algorithm used in our case.[18] Here, we used $1/(f_{(meas)}^{(i)})^2$ as the weighting factor. There are detailed descriptions about the LM algorithm in the literature.[19,20]

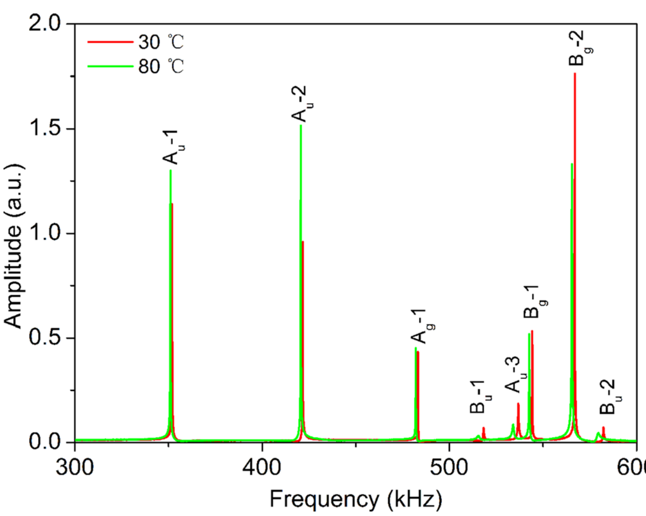

FIG. 2. Measured resonant modes from 300 kHz to 600 kHz at 30 °C and 80 °C. The peaks shifted to lower frequencies with the increase in temperature.

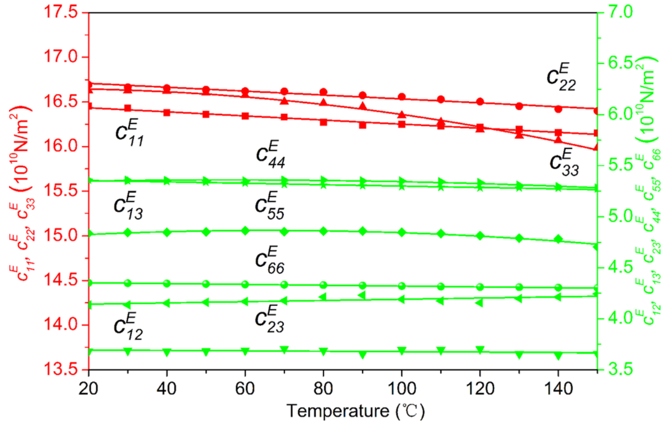

FIG. 3. Temperature dependence of elastic stiffness constants c_{11}^E, c_{12}^E, c_{13}^E, c_{22}^E, c_{23}^E, c_{33}^E, c_{44}^E, c_{55}^E, and c_{66}^E. The left (red) and right (green) y-axes are for (c_{11}^E, c_{22}^E, and c_{33}^E) and (c_{12}^E, c_{13}^E, c_{23}^E, c_{44}^E, c_{55}^E, and c_{66}^E), respectively. Elastic constants (c_{11}^E, c_{12}^E, c_{22}^E, c_{23}^E, c_{55}^E, and c_{66}^E) were fitted to a linear function of temperature, while (c_{13}^E, c_{33}^E, and c_{44}^E) were fitted to a quadratic function of temperature.

Finally, the elastic and piezoelectric constants of KTP were obtained as a function of temperature. Figures 3 and 4 show the temperature dependence of the 9 elastic constants and 4 piezoelectric constants of KTP, respectively. The points correspond to experimental results while the lines are least-squares fitting curves.

A summary of the results for elastic and piezoelectric constants together with the fitted results of $\varepsilon_{11}^S/\varepsilon_0$, $\varepsilon_{22}^S/\varepsilon_0$, and $\varepsilon_{33}^S/\varepsilon_0$ are shown in Tables I and II. Elastic constants (c_{11}^E, c_{12}^E, c_{22}^E, c_{23}^E, c_{55}^E, and c_{66}^E) were all fitted into a linear function of temperature, while (c_{13}^E, c_{33}^E, and c_{44}^E) were fitted to a quadratic function of temperature because their experimental data showed some curvatures. All piezoelectric constants were fitted to quadratic functions of temperature. A summary of fitted functions of the elastic and piezoelectric constants is shown in Table III. All elastic constants, except

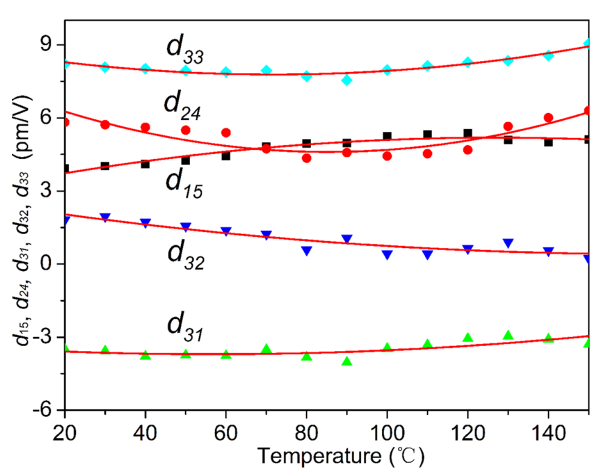

FIG. 4. Temperature dependence of piezoelectric stress constants d_{15}, d_{24}, d_{31}, d_{32}, and d_{33}. All piezoelectric constants were fitted to quadratic functions of temperature.

TABLE I. RUS results of elastic constants c_{ij} (10^{10} N/m^2) at some selected temperatures, and comparison with existing data in the literatures at room temperature (RT).

T (°C)	c^E_{11}	c^E_{12}	c^E_{13}	c^E_{22}	c^E_{23}	c^E_{33}	c^E_{44}	c^E_{55}	c^E_{66}	Reference
20	16.454	3.678	4.836	16.694	4.134	16.628	5.359	5.357	4.352	This work
40	16.378	3.687	4.848	16.655	4.153	16.624	5.353	5.344	4.345	This work
60	16.341	3.688	4.864	16.622	4.168	16.576	5.349	5.328	4.336	This work
80	16.273	3.687	4.859	16.612	4.212	16.694	5.358	5.307	4.329	This work
100	16.247	3.693	4.848	16.559	4.189	16.487	5.348	5.393	4.319	This work
120	16.219	3.703	4.814	16.504	4.155	16.191	5.333	5.282	4.310	This work
140	16.157	3.643	4.783	16.420	4.212	16.069	5.293	5.278	4.305	This work
Measured at RT	17.11	…	…	16.98	…	17.39	5.28	5.58	4.40	This work
KTP	16.367	3.481	4.153	16.322	4.389	16.455	5.201	5.399	4.491	21 (RT)
KTP	17.67	5.313	3.89	16.27	3.76	14.61	4.007	4.97	5.332	1 (RT)
KTP	17	3.333	4.0	17.4	3.5	14.95	5.919	5.454	4.313	5 (RT)
KTP	16.601	…	…	16.409	…	…	5.193	5.143	4.284	22 (RT)
Fe:KTP	16.74	3.52	4.70	16.49	4.75	18.26	5.43	5.46	4.28	23 (RT)

TABLE II. RUS results of piezoelectric constants d_{ij} (pm/V), fitted results of relative dielectric constants at selected temperatures, and existing data in the literatures at room temperature (RT).

	Inversion results					Fitted results			
T(°C)	d_{15}	d_{24}	d_{31}	d_{32}	d_{33}	$\varepsilon^S_{11}/\varepsilon_0$	$\varepsilon^S_{22}/\varepsilon_0$	$\varepsilon^S_{33}/\varepsilon_0$	Reference
20	3.919	5.821	−3.490	1.810	8.203	11.210	11.104	15.897	This work
40	4.100	5.616	−3.784	1.720	8.013	11.241	11.116	16.111	This work
60	4.420	5.390	−3.758	1.386	7.873	11.291	11.131	16.111	This work
80	4.939	4.341	−3.823	0.585	7.710	11.351	11.149	16.254	This work
100	5.247	4.427	−3.466	0.421	7.954	11.405	11.171	16.618	This work
120	5.369	4.681	−3.054	0.643	8.278	11.448	11.201	16.830	This work
140	4.991	6.010	−3.084	0.554	8.552	11.471	11.241	17.088	This work
KTP	−1.5	−2.1	9.3	4.0	4.6	11.6	11.0	15.4	24, 25 (RT)
KTP	…	…	…	…	15.2	…	…	…	26 (RT)
KTP	5.41	0.61	3.82	11.1	25.8	10.14	14.18	12.87–14.62	22 (RT)

TABLE III. Fitted functions of the temperature dependence of elastic and piezoelectric constants.

Temperature dependence of elastic constants (10^{10} N/m^2)	Temperature dependence of piezoelectric constants (pm/V)
$c^E_{11} = 16.482 - 2.3 \times 10^{-3}T$	$d_{15} = 3.121 + 3.256 \times 10^{-2}T - 1.283 \times 10^{-4}T^2$
$c^E_{12} = 3.695 - 1.945 \times 10^{-4}T$	$d_{24} = 7.438 - 6.66 \times 10^{-2}T + 3.904 \times 10^{-4}T^2$
$c^E_{13} = 4.784 + 2.52 \times 10^{-3}T – 1.918 \times 10^{-5}T^2$	$d_{31} = -3.428 - 9.65 \times 10^{-3}T + 8.546 \times 10^{-5}T^2$
$c^E_{22} = 16.753 - 2.19 \times 10^{-3}T$	$d_{32} = 2.519 - 2.543 \times 10^{-2}T + 7.66 \times 10^{-5}T^2$
$c^E_{23} = 4.131 - 5.952 \times 10^{-4}T$	$d_{33} = 8.746 - 2.715 \times 10^{-2}T + 1.891 \times 10^{-4}T^2$
$c^E_{33} = 16.649 + 4.840 \times 10^{-4}T - 3.377 \times 10^{-5}T^2$	
$c^E_{44} = 5.333 - 9.527 \times 10^{-4}T - 8.609 \times 10^{-6}T^2$	
$c^E_{55} = 5.368 - 6.872 \times 10^{-4}T$	
$c^E_{66} = 4.361 - 4.034 \times 10^{-4}T$	

c^E_{23}, increase with temperature. At room temperature, our elastic constants compared well with those published data in Table I,[2,5,21–23] while the temperature dependence data had never been measured before. The temperature dependence of the 5 piezoelectric constants is shown in Figure 4. The piezoelectric constants only have small changes with temperature in the temperature range of 20 °C to 150 °C. Because the Curie temperature of KTP single crystal is about 936 °C, which is far above our experiment temperature range, the spontaneous polarization as well as piezoelectric properties does not show drastic changes in the experimental temperature range of 20 °C to 150 °C. The RUS result of the piezoelectric constant d_{33} at 20 °C is about 8.203 pm/V, which corresponds well with direct measurement result using a d_{33} PiezoMeter. On the other hand, the literature data of d_{33} vary from 4.6 pm/V to 25.2 pm/V.[22,24–26] One critical judgment is the Poisson's ratio test, which should not be negative. In Refs. 22 and 25, d_{31}, d_{32}, and d_{33} were all positive, which means that the crystal will expand in all three dimensions under a field along the poling direction. This will lead to a

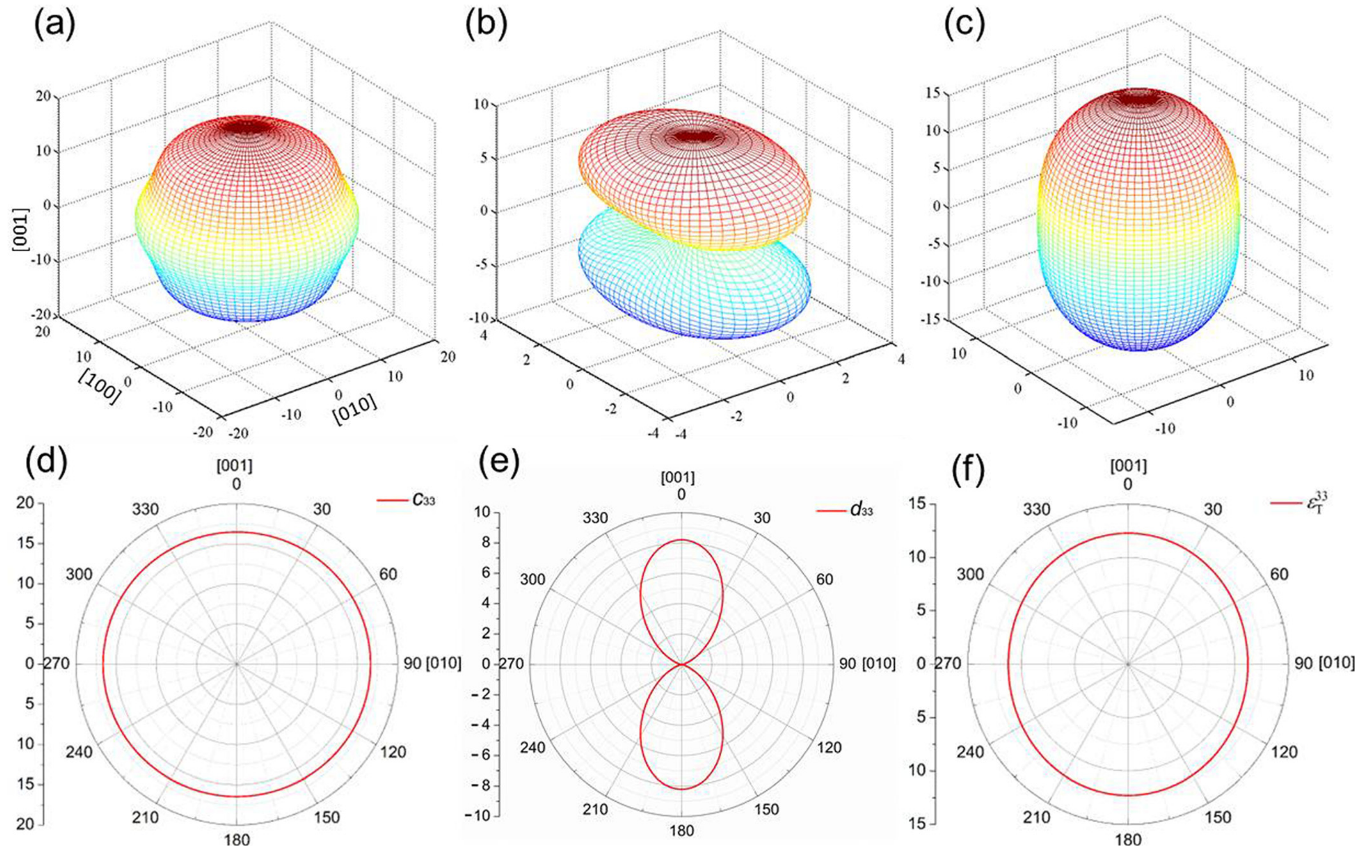

FIG. 5. Orientation dependence of (a) c_{33}; (b) d_{33}; (c) ε_{33}; and the cross section plots of (d) c_{33}; (e) d_{33}; (f) ε_{33} in the [001]-[010] plane of the KTP single crystal.

negative Poisson's ratio; hence, those literature results are in question.

To illustrate the orientation dependence of these physical properties, coordinate transformation has been performed on the obtained single domain data sets. The constants, c_{33}, d_{33}, and ε_{33}, were rotated counterclockwise first around the x-axis by an angle α, then rotated counterclockwise around the new z'-axis by an angle γ in the 3-dimensional space. The corresponding parameters in the 3-dimensional space as functions of α and γ are shown in Figure 5. The elastic constant c_{33} reaches its maximum value at $\beta = 90°$, while the maximum values of d_{33} and ε_{33} all appear at $\beta = 0°$.

A rectangular parallelepiped KTP sample has a macroscopic symmetry of C_{2h}, so that there are four groups of vibration modes denoted by A_g, A_u, B_g, and B_u.[16,27] The temperature dependence of four selected mode frequencies A_u-2, B_g-1, A_g-15, and B_u-13 are shown in Figure 6. The points correspond to the measured results, while the lines are calculated results using our obtained material constants. One can see that the calculated and measured results are in excellent agreement.

In order to check the self-consistency of the obtained tensor properties, the measured free dielectric constants ε_{11}^T and ε_{22}^T are compared to those calculated values in the given temperature range using the following formulas:

$$\varepsilon_{11}^T = \varepsilon_{11}^S + d_{15}e_{15}, \tag{2}$$

$$\varepsilon_{22}^T = \varepsilon_{22}^S + d_{24}e_{24}, \tag{3}$$

where

$$e_{15} = d_{15}c_{55}^E, \tag{4}$$

$$e_{24} = d_{24}c_{44}^E. \tag{5}$$

Also, we have used different formulas to calculate the piezoelectric constants d_{15} and d_{24} to check the self-consistency of the matrix data

$$d_{15} = k_{15} \times \sqrt{\varepsilon_{11}^{\mathrm{T}} \times s_{55}^{\mathrm{E}}}, \tag{6}$$

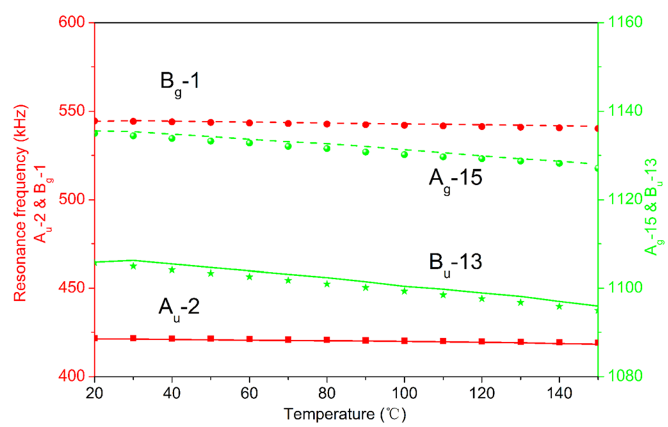

FIG. 6. Resonance frequencies of modes A_u-2, B_g-1, A_g-15, and B_u-13 versus temperature, where the solid and dashed lines are calculated results while the points correspond to directly measured results. The left and right y-axes are for (A_u-2, B_g-1) and (A_g-15, B_u-13), respectively.

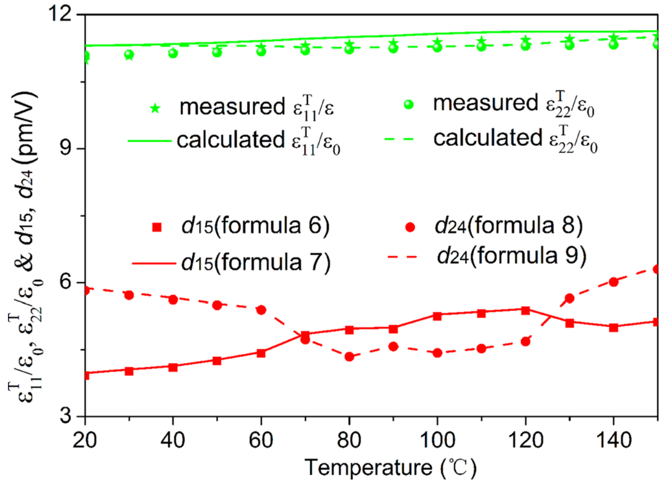

FIG. 7. Measured (points) and calculated (solid and dashed lines) relative dielectric constants, $\varepsilon_{11}^T/\varepsilon_0$ and $\varepsilon_{22}^T/\varepsilon_0$, together with d_{15} and d_{24} calculated using different formulas, as functions of temperature.

$$d_{15} = e_{15} \times s_{55}^{\mathrm{E}}, \tag{7}$$

$$d_{24} = k_{24} \times \sqrt{\varepsilon_{11}^{\mathrm{S}} \times s_{44}^{\mathrm{E}}}, \tag{8}$$

$$d_{24} = e_{24} \times s_{44}^{\mathrm{E}}, \tag{9}$$

where s_{44}^E and s_{55}^E are elastic stiffness constants, k_{15} and k_{24} are electromechanical coupling factors, which can be obtained from the following formulas:

$$k_{15} = \sqrt{(c_{55}^D - c_{55}^E)/c_{55}^D}, \tag{10}$$

$$c_{55}^D = c_{55}^E + e_{15}^2 \varepsilon_{11}^S, \tag{11}$$

$$k_{24} = \sqrt{(c_{44}^D - c_{44}^E)/c_{44}^D}, \tag{12}$$

$$c_{44}^D = c_{44}^E + e_{24}^2 \varepsilon_{22}^S. \tag{13}$$

The measured and calculated $\varepsilon_{11}^T/\varepsilon_0$ and $\varepsilon_{22}^T/\varepsilon_0$ together with d_{15} and d_{24} calculated using different formulas are shown in Figure 7. In the temperature range from 20 °C to 150 °C, the relative errors $|(\varepsilon_i^T(cal) - \varepsilon_i^T(meas))/\varepsilon_i^T(meas)|$ $(i = 11, 22)$ between the measured and calculated results are below 2.9% and 2.0%, respectively. And the relative errors of d_{15} and d_{24} calculated by different formulas are below 1.5% and 1.0%, respectively. Generally, the full matrix constants can be considered self-consistent if the deviation of the calculated result of each constant using different formulas was less than 5%.[28] To further check the self-consistency, we also compared the elastic stiffness constants c_{11}^E, c_{22}^E, c_{44}^E, c_{55}^E, and c_{66}^E determined by the RUS technique with those directly measured ones by the ultrasonic pulse-echo method, as shown in Table I. From our analysis, the overall errors of the RUS technique are less than 4.0%.

IV. CONCLUSIONS

In summary, the dielectric, elastic, and piezoelectric constants of the KTP single crystal have been determined using only one sample from room temperature up to 150 °C by an extended RUS technique. We have achieved two goals in this investigation: (1) extended the RUS technique to characterize an orthorhombic symmetry system for which 17 independent constants can be determined from only one sample; (2) obtained the temperature dependent full tensor properties of KTP single crystals with high self-consistency from room temperature up to 150 °C. Our results show that the elastic constants (c_{11}^E, c_{13}^E, c_{22}^E, and c_{33}^E) and piezoelectric constants (d_{15}, d_{24}, and d_{32}) of KTP single crystal are strongly temperature dependent, while the remaining constants are nearly independent of temperature. Using the full set material constants, we were able to calculate the orientation dependence of the piezoelectric, elastic, and dielectric constants, which can help determine the optimum cut of the crystal for desired applications.

ACKNOWLEDGMENTS

This work was supported by the National Natural Science Foundation of China (Grant Nos. 31430031, U1332118, and 11374245), the Natural Science Foundation of Fujian Province (Grant No. 2013J01163), and the NIH under the Grant No. P41-EB21820.

[1]I. I. Zubrinov, V. K. Sapozhnikov, E. V. Pestrykov, and V. V. Atuchin, Proc. SPIE **5129**, 249–254 (2003).
[2]N. I. Sorokinaa and V. I. Voronkova, Crystallography Reports **52**(1), 80–93 (2007).
[3]M. N. Satyanarayan, A. Deepthy, and H. L. Bhat, Crit. Rev. Solid State Mater. Sci. **24**, 103–191 (1999).
[4]M. Roth, *Springer Handbook of Crystal Growth* (Springer Berlin, 2010), pp. 691–723.
[5]D. K. T. Chu, J. D. Bierlein, and R. G. Hunsperger, IEEE Trans. Ultrason., Ferroelectr., Freq. Control **39**, 683–687 (1992).
[6]M. Lei, J. L. Sarrao, W. M. Visscher, T. M. Bell, J. D. Thompson, A. Migliori, U. W. Welp, and B. W. Veal, Phys. Rev. B **47**, 6154 (1993).
[7]G. Liu, S. J. Zhang, W. H. Jiang, and W. W. Cao, Mater. Sci. Eng. R **89**, 1–48 (2015).
[8]L. G. Tang and W. W. Cao, Appl. Phys. Lett. **106**, 052902 (2015).
[9]Y. Zhang, H. Y. Wang, C. Q. Ma, Y. W. Jia, J. Li, J. Y. Wang, R. Boughton, and H. D. Jiang, J. Cryst. Growth **412**, 67–71 (2015).
[10]Y. Zhang, J. Li, X. Z. Cao, J. Yang, J. Y. Wang, and H. D. Jiang, AIP Adv. **4**, 127103 (2014).
[11]D. P. Shumov, V. S. Nikolov, K. N. Iliev, and A. L. Aleksandrovskii, Cryst. Res. Technol. **25**, 1245–1250 (1990).
[12]Y. Nakanishi, T. Kumagai, M. Yoshizawa, K. Matsuhira, S. Takagi, and Z. Hiroi, Phys. Rev. B **83**, 184434 (2011).
[13]R. J. Jiménez-Riobóo, M. García-Hernández, C. Prieto, J. J. Fuentes-Gallego, E. Blanco, and M. Ramírez-delSolar, J. Appl. Phys. **81**, 7739 (1997).
[14]F. Willis, R. G. Leisure, and I. Jacob, Phys. Rev. B **50**, 13792 (1994).
[15]E. P. Eer Nisse, IEEE Trans. Sonics Ultrason. **14**, 153–159 (1967).
[16]I. Ohno, Phys. Chem. Miner. **17**, 371–378 (1990).
[17]B. J. Zadler, J. H. L. Le Rousseau, J. A. Scales, and M. L. Smith, Geophys. J. Int. **156**, 154–169 (2004).
[18]A. Migliori and J. L. Sarrao, *Resonant Ultrasound Spectroscopy: Applications to Physics, Materials Measurements, and Nondestructive Evaluation* (Wiley-Interscience, 1997).
[19]J. Pujol, Geophysics **72**, 1–16 (2007).
[20]J. J. Moré, B. S. Garbow, and K. E. Hillstrom, Argonne National Laboratories Report No. ANL-80-74, 1980.
[21]Y. S. Yu, B. M. Jin, J. H. Kim, J. I. Lee, I. S. Kim, H. S. Hwang, and S. C. Kim, J. Korean Phys. Soc. **32**, S518–S520 (1998).
[22]I. M. Sil'vestrova, V. A. Maslov, and Yu. V. Pisarevskii, Kristallografiya **37**, 1227–1231 (1992).

[23]L. P. Shi, T. C. Chong, and X. W. Xu, J. Cryst. Growth **198–199**, 551–554 (1999).
[24]Z. L. Gao, Y. X. Sun, X. Yin, S. P. Wang, M. H. Jiang, and X. T. Tao, J. Appl. Phys. **108**, 024103 (2010).
[25]J. D. Bierlein and C. B. Arweiler, Appl. Phys. Lett. **49**, 917 (1986).
[26]H. Graafsma, G. W. J. C. Heunen, S. Dahaoui, A. E. L. Haouzi, N. K. Hansen, and G. Marnier, Acta Cryst. B **53**, 565–567 (1997).
[27]A. S. Davydov, *Theory of Absorption Spectra of Molecular Crystals* (Department of Chemistry, University of California, 1949).
[28]V. Y. Topolov and C. R. Bowen, J. Appl. Phys. **109**, 094107 (2011).